Peierls Structure of $(H_3O)_{0.33}Li_{0.8}[Pt(mnt)_2]\cdot 1.67H_2O$

Akiko KOBAYASHI,* Takehiko MORI, Yukiyoshi SASAKI, Hayao KOBAYASHI,†
M. M. AHMAD,†† and A. E. UNDERHILL††

Department of Chemistry, Faculty of Science, The University of Tokyo, Hongo, Tokyo 113
†*Department of Chemistry, Faculty of Science, Toho University, Funabashi, Chiba 274*
††*Department of Chemistry, University College of North Wales, Bangor, Gwynedd LL57 2UW, U.K.*

(Received June 9, 1984)

The crystal structure determination of the title compound (abbreviated as α-LiPt(mnt) has been performed at room temperature and 153 K. The $[Pt(mnt)_2]^{n-}$ (mnt=1,2-dicyano-1,2-ethylenedithiolato, $C_4N_2S_2^{2-}$) anions stack face-to-face along the c-axis with Pt···Pt distance of 3.6 Å. The room temperature structure and the average structure of the 153 K superstructure are almost the same. The room temperature conductivity of α-LiPt(mnt) is about 200 S cm^{-1}, and the compound undergoes a metal-insulator transition (Peierls transition) at 220 K. In α-LiPt(mnt) the conduction pathway is through the ligand-centered π-system which is composed of predominantly S $3p_z$ orbitals. Oscillation photographs about the c-axis show strong satellite spots on the layerlines of $(0.41+n)c^*$ and $(0.59+n)c^*$ (n=0, ±1, ±2, ···). The content of Li cation reveals that these satellite spots can be described as $2k_F$ spots. The regular appearance of characteristic satellite reflections indicates that α-LiPt(mnt) has a sinusoidally modulated lattice. The wave vector of the lattice modulation wave is $\mathbf{k}=0.15\mathbf{b}^*+0.59\mathbf{c}^*$ and the amplitude of the lattice modulation wave is $0.045\,\boldsymbol{a}/a+0.13\boldsymbol{b}/b+0.060\boldsymbol{c}/c$ Å. The overlap integrals along face-to-face stacking directions are much larger than the interstack overlap integrals and the resulting large anisotropy indicates that α-LiPt(mnt) is a one-dimensional metal.

The crystal structures, syntheses and electrical conduction properties of 1,2-dithiolene complexes have been extensively studied.[1-3] Recently a new type one-dimensional partially oxidized $[M(mnt)_2]^{n-}$ (M= Ni, Pd, Pt; mnt=1,2-dicyano-1,2-ethylenedithiolato, $C_4N_2S_2^{2-}$) complex has been reported.[4,5] Metallic behavior has been found for crystals of $(H_3O)_{0.33}Li_{0.8}[Pt(mnt)_2]\cdot 1.67H_2O$, which is abbreviated as α-LiPt(mnt).[4-6]† Its room temperature conductivity, 200 S cm^{-1} is as large as that of $K_2[Pt(CN)_4]\cdot Br_{0.3}\cdot 3.2H_2O$ (KCP(Br)). Although the $[Pt(mnt)_2]^{n-}$ anions stack face-to-face with a Pt···Pt distance of 3.639 Å, the partially oxidized 1,2-dithiolene complexes have a conduction pathway based on the ligand-centered π-system (predominantly sulfur $3p_z$ orbitals). This is in contrast to the high conductivity of inorganic one-dimensional metals containing tetracyano-platinate and bis(oxalato)platinate anions which arises from a partially occupied Pt $5dz^2$ electron energy band.

α-LiPt(mnt) undergoes a metal-insulator transition at about 220 K.[4] The static magnetic susceptibility of α-LiPt(mnt) has been measured from 2—300 K by J. R. Cooper *et al.*[6] Above 150 K, the conduction electron paramagnetism $X_p=X_s-C/T$ gradually develops. It shows a sharp knee at 220 K corresponding to metal-semiconductor phase transition.

In this paper we report the crystal structures of α-LiPt(mnt) at room temperature and at 153 K. The 153 K superstructure corresponds to a so-called Peierls structure.

Experimental

Crystal Preparation, Data Collection, and Structure Solution. Slow aerial oxidation of a 50% aqueous acetone solution of $H_2[Pt(mnt)_2]$ and LiCl gave $Li_xH_y[Pt(mnt)_2]\cdot nH_2O$ as a black microcrystalline product containing small shining black needle crystals (α-LiPt(mnt))[7] and plate crystals (β-LiPt(mnt)).[8] The needle crystals were used in this experiment. Details concerning crystal characteristics and X-ray diffraction methodology are shown in Table 1. Intensities were measured on a Rigaku automated four-circle diffractometer with Mo $K\alpha$ radiation at room temperature and at 153 K. Graphite-monochromatized Mo $K\alpha$ radiation (0.71073 Å) was used for data collection. Intensities were collected by using a $\omega-2\theta$ scan technique. The scan width was determined for each reflection according to the formula $w=(A+B\tan\theta)°$. Three standard reflections monitored every 50

Table 1. Crystal and refinement data for α-LiPt(mnt)

	At room temperature	At 153 K
Formula weight	517.52	517.52
a/Å	15.596(4)	15.564(4)
b/Å	6.410(3)	6.320(3)
c/Å	3.639(2)	5.597(1)
α/°	100.52(9)	99.35(2)
β/°	90.75(5)	90.54(2)
γ/°	96.28(6)	96.25(3)
V/Å^3	355.3(2)	346.9(1)
Space group	$P\bar{1}$	$P\bar{1}$
Z	1	1
d_{calc}/g·cm^{-3}	2.418	2.418
Crystal dimension/mm^3	0.04×0.25×0.38	0.031×0.2×0.35
μ/cm^{-1}	112.12	112.12
$2\theta_{max}$/°	60	60
Number of independent reflections $\|F_o\|>3\sigma(\|F_o\|)$	1686	2015
Parameters	96	96
R_w	0.065	0.068
Standard reflections	3	3
Scan	$2\theta-\omega$	$2\theta-\omega$
$A+B\tan\theta$	$1.2+0.6\tan\theta$	$1.24+0.5\tan\theta$
Scan speed 2θ/°	2°/min	4°/min
Background/sec	10	5

† This compound was initially reported to be $Li_x[Pt(mnt)_2]\cdot 2H_2O$ (where $x\approx 0.8$) but has recently been shown to contain protons in the lattice.[7]

(at room temperature) and every 100 (at 153 K) measurements, and their intensities remained essentially constant during the data collection. The data was corrected for Lorentz and polarization. The crystal was covered with epoxy resin for measurements at room temperature and was sealed in a glass capillary for measurements at 153 K. At 153 K, the relatively weak satellite reflections were observed, but these were not included in the analyses of the average structure. The structure was solved by the heavy-atom method and refined to $R=0.065$ and $R=0.068$, $w=1/[\sigma^2+0.01|F_o|^2]$ for $|F_o|\geqq 15$, $w=0.2$ for $|F_o|<15$ using 1686 and 2015 independent reflections for which $I>3\sigma(I)$ at room temperature and at 153 K, respectively. Absorption corrections were performed in both cases, but did not result in much improvement of the room temperature structure because the crystal used for the data collection was twinned.

The c*-axis projection of the structure of α-LiPt(mnt) is shown in Fig. 1. Atomic parameters are shown in Table 2. The thermal parameters and F_o-F_c tables are kept at the office of this Bulletin as Document No. 8451.

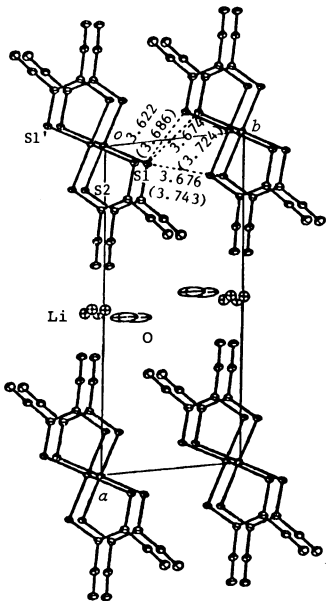

Fig. 1. The c*-axis projection of the average structure of α-LiPt(mnt) at 153 K. The intermolecular distances in parentheses are those at room temperature.

Table 2. Atomic parameters (×10000)

	X	Y	Z	B/Å²
a) At room temperature				
Pt	0	0	0	2.8(0)
S_1	708(2)	3322(5)	1946(10)	3.7(1)
S_2	1276(2)	−1377(5)	−865(10)	3.7(1)
C_1	1765(7)	2854(17)	1685(34)	3.1(3)
C_2	2012(7)	881(18)	459(37)	3.5(3)
C_3	2416(7)	4586(18)	2854(38)	3.8(4)
C_4	2925(7)	626(18)	200(42)	4.3(4)
N_1	2958(7)	5913(18)	3796(39)	6.0(4)
N_2	3633(6)	475(17)	29(42)	6.2(4)
O	4753(7)	7614(33)	4695(91)	23.4(13)
Li*	499(4)	18(11)	88(15)	3.9(10)
b) At 153 K				
Pt	0	0	0	1.6(0)
S_1	700(2)	3335(5)	1981(10)	2.1(1)
S_2	1284(2)	−1371(5)	−846(10)	2.0(1)
C_1	1761(8)	2845(22)	1727(36)	2.0(3)
C_2	2003(8)	852(19)	431(33)	1.7(3)
C_3	2407(8)	4617(23)	2940(40)	2.4(3)
C_4	2910(9)	627(22)	271(42)	2.4(3)
N_1	2963(9)	6015(22)	3919(43)	3.5(4)
N_2	3644(8)	514(21)	102(43)	3.2(3)
O	4742(13)	8007(52)	4076(101)	14.6(15)
Li*	496(6)	19(15)	66(22)	3.4(13)

* The occupancy probability is 0.40.

Results and Discussions

The Room Temperature Structure and the Average Structure of the 153 K Superstructure. The crystal structures of α-LiPt(mnt) at both temperatures are almost the same. The planar $[Pt(mnt)_2]^{n-}$ anions stack face-to-face along the c-axis with an eclipsed configuration to form a columnar stacked structure. The interplanar distance between the $[Pt(mnt)_2]^{n-}$ anions are 3.592 and 3.537 Å, and the Pt···Pt distances are 3.639 and 3.597 Å, at room temperature and at 153 K respectively. In α-LiPt(mnt), all the inter-anion distances within the stack are equal. This is different from the structures found for the similar $[Pt(mnt)_2]$ complexes $Rb[Pt(mnt)_2]\cdot 2H_2O$[9] and β-LiPt(mnt),[8] both of which possess dimeric structures. In $Rb[Pt(mnt)_2]\cdot 2H_2O$ the interplanar spacing within the dimer is 3.356 Å and between dimers 3.512 Å. In β-LiPt(mnt) the interplanar spacing within the dimer is 3.346 Å and between dimers 3.631 Å and 3.643 Å. In both compounds the anions are arranged along the column in a fully eclipsed configuration, which is a characteristic of $M_x[Pt(mnt)_2]$ compounds containing small cations. Mono-anion salts with bulky organic cations often pos-

Table 3. Comparison of bond lengths (l/Å) and angles (φ/°) in $[Pt(mnt)_2]^{n-}$ anions

	α-LiPt(mnt) (R. T.)	α-LiPt(mnt) (153 K)
Pt-S	2.271(2)	2.267(3)
S-C	1.722(8)	1.705(10)
C-C (inner ring)	1.360(16)	1.365(18)
C-C	1.436(11)	1.433(14)
C-N	1.123(11)	1.115(16)
SPtS α	90.4(1)	90.3(1)
PtSC β	102.2(3)	102.0(4)
SCC γ	122.8(6)	122.8(7)
SCC δ	118.3(6)	118.3(7)
CCC ε	119.0(7)	118.9(8)
CCN φ	117.9(8)	177.5(11)

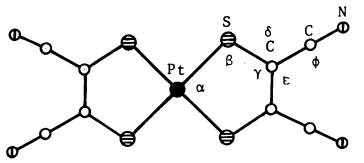

sess columnar stacks containing anion dimers with a staggered configuration.[10] The $[Pt(mnt)_2]^{n-}$ anion is almost planar with average bond lengths (in Å) Pt–S 2.271(2), 2.267(3), S–C 1.722(8), 1.705(10), and C–C 1.360(16), 1.365(18), at room temperature and at 153 K, respectively. The bond lengths and angles are compared in Table 3.

In $Rb_{1.67}[Pt(C_2O_4)_2]\cdot 1.5H_2O$,[11] intermolecular distances are much shortened by the formation of the Pt···Pt bonds. The Pt···Pt distances are modulated by the Peierls distortion and the molecular plane is concave in order to reduce the steric hindrance with the ligands of the neighbouring molecules. Terminal oxygen atoms of the ligands are deviated 0.4—0.5 Å from the plane. However, in α-LiPt(mnt) the molecule is almost planar both at room temperature and at 153 K probably because of the large intermolecular separation. The equations of the best planes and the perpendicular distances from these planes are deposited and kept at the office of this Bulletin.

Intermolecular short contacts are also shown in Fig 1. The transverse interatomic distances between the S atoms are considerably shortened in the low temperature. Close S···S contacts of less than 3.8 Å are shown in Table 4. The short interatomic distances between the S atoms on adjacent molecules in adjacent stacks are 3.686, 3.724, and 3.743 Å at room temperature and 3.622, 3.674, and 3.676 Å at 153 K. Close S···S contacts in the transverse direction of the Pt chain have been also found in α-LiPt(mnt) and $Rb[Pt(mnt)_2]\cdot 2H_2O$. There are two Li sites in the unit cell. The Li ions are disordered and the occupancy probability of the Li site is 40%. The Li ions are six-coordinated and Li···N(O) distances vary from 1.94 to 2.69 Å at room temperature and 2.06 to 2.54 Å at 153 K. There are two oxygen atoms and $0.8Li^+$ cations in the unit cell. They are located in-between the $[Pt(mnt)_2]$ anions along the a-axis. As mentioned before, the results of the chemical analysis of α-LiPt(mnt) have shown that the unit cell should contain 0.33 H_3O^+ but the crystal structure analyses could not distinguish the sites of H_3O^+ from those of H_2O. Table 5 lists short interatomic distances of less than 3.0 Å within the coordination spheres around the Li cation and the oxygen atom of the water molecule (or hydroxonium ion).

Measurements of satellite reflections by oscillation photographs. We examined temperature dependence of intensities of X-ray reflections within the temperature range between 90 K and 300 K. An oscillation photograph around the c-axis shows that the strong satellite spots appear on the layer lines of $(0.41+n)c^*$, or $(0.59+n)c^*$ ($n=0, \pm1, \cdots$) (Fig. 2). The cation content revealed that these satellite spots can be described as $2k_F$ spots.[7] The satellite reflections show that α-LiPt(mnt) has a sinusoidally modulated lattice. Figure 3 shows the temperature dependence of intensities of the satellite spots ($\xi\ \eta\ \zeta$). The intensities of satellite reflections, (−13, −2.85, −0.41), (6, 3.85, 0.41), and (13, 2.15, 0.59)

TABLE 4. THE SHORT INTERATOMIC DISTANCES (l/Å) BETWEEN S ATOMS LESS THAN 3.8 Å

	At room temperature	At 153 K
$S_1\cdots S_1$[a]	3.639(8)	3.597(7)
$S_1\cdots S_2$[b]	3.743(5)	3.676(5)
$S_1\cdots S_1$[c]	3.686(7)	3.622(7)
$S_1\cdots S_2$[d]	3.724(7)	3.674(7)

Symmetry codes

a)	x,	y,	$1+z$
b)	x,	$1+y$,	z
c)	$-x$,	$1-y$,	$-z$
d)	$-x$,	$1-y$,	$1-z$

TABLE 5. SHORT INTERATOMIC DISTANCES (l/Å) WITHIN THE COORDINATION SPHERES TO 3.0 Å AROUND THE Li CATIONS AND OXYGEN ATOMS OF WATER MOLECULES

	At room temperature	At 153 K
Li···Li[a]	0.65(10)	0.52(16)
Li···O[b]	1.94(6)	2.06(8)
Li···N_2[c]	2.17(7)	2.09(10)
Li···N_2[a]	2.25(7)	2.28(10)
Li···O[d]	2.34(7)	2.00(10)
Li···O[e]	2.53(6)	2.22(10)
Li···O[f]	2.69(7)	2.54(8)
O···N_1[c]	2.88(2)	2.91(3)
O···O[g]	(>3.0)	2.54(6)

Symmetry code

a)	$1-x$,	$-y$,	$-z$
b)	$1-x$,	$1-y$,	$1-z$
c)	x,	y,	z
d)	x,	$-1+y$,	z
e)	x,	$-1+y$,	$-1+z$
f)	$1-x$,	$1-y$,	$-z$
g)	$1-x$,	$2-y$,	$1-z$

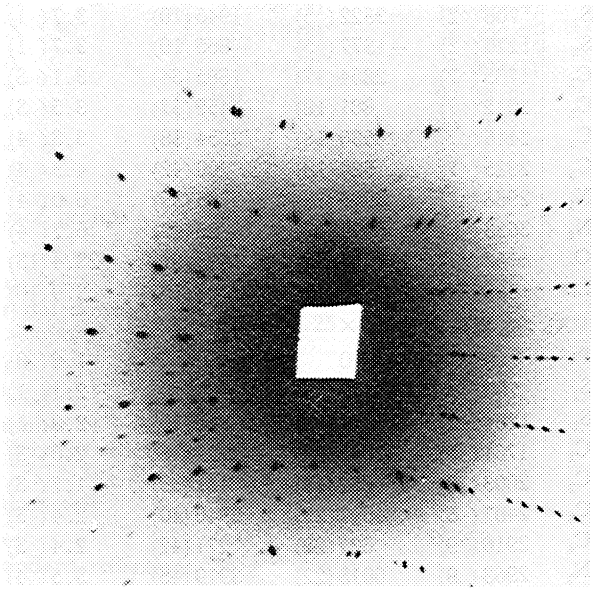

Fig. 2. An oscillation photograph around the c-axis at 153 K. Strong satellite spots appear on the layer lines of $(0.41\pm n)$ c* or $(0.59\pm n)c^*$ ($n=0,1,\cdots$).

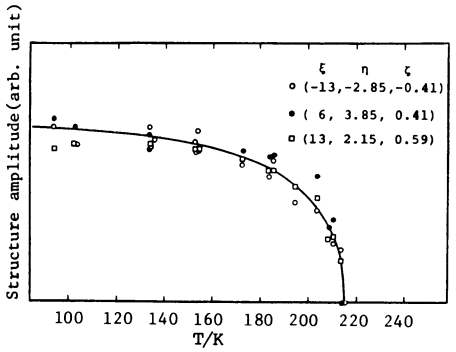

Fig. 3. Temperature dependence of the intensities of satellite reflections between the temperature range of 90 K–300 K.

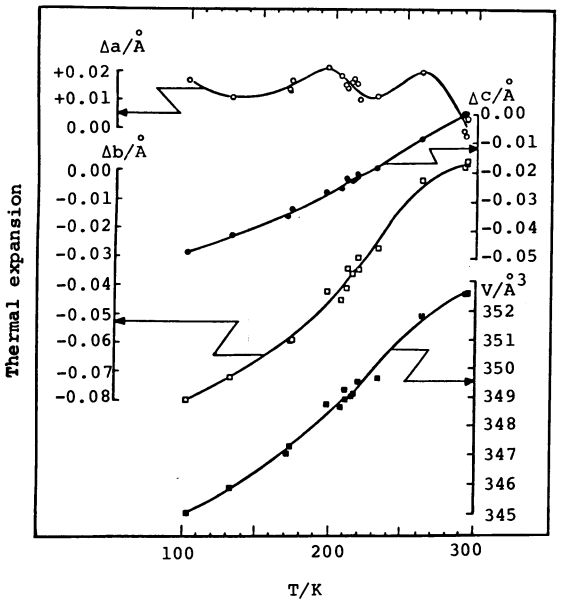

Fig. 4. Temperature dependence of the cell parameters.

were measured under the same conditions as the main reflections. The intensities are roughly proportional to $\sqrt{T-T_c}$ (T_c=213 K).

Temperature Dependence of the Cell Parameters. The temperature dependence of the cell parameters are shown in Fig. 4. The cell constants b and c are shortened by 8 and 5% within the temperature range between 300 K and 90 K and a is expanded by up to 2%.

It is worth noticing that the contraction of the transverse direction b, is larger than the change in a and c. The stack of the $[Pt(mnt)_2]$ complexes is parallel to the c axis. The large contraction of b indicates that the S···S interaction in the transverse direction of complexes are strengthened in the low temperature.

The Analysis of the Modulation wave in the Peierls Structure. As is well-known, the one-dimensional metallic state is not stable at low temperature. The system tends to be distorted periodically in order to gain electronic energy. The lattice instability brings about the superstructure and characteristic X-ray diffuse scatterings appear below transition temperature (T_c). The lattice-modulation wave with the wave number of $2k_F$ develops below T_c.

When the lattice is sinusoidally modulated, the position of the j-th atom of the n-th cell, $\mathbf{r}_{jn}$, is given by $\mathbf{r}_{jn}=\mathbf{R}_n+\mathbf{d}_j+\mathbf{P}\sin(2\boldsymbol{k}_F\cdot\mathbf{R}_n)$, where $\mathbf{R}_n$ is the lattice vector of the n-th lattice point of the average structure, $\mathbf{P}$ is an amplitude of the modulation wave, and $\boldsymbol{k}_F$ is the wave vector of the modulation wave. The intensity formula of X-ray diffraction by the crystal with sinusoidal modulation waves whose fundamental lattice contains only one molecule, is as follows

$$I(\xi\eta\zeta) = |F(\xi\eta\zeta)|^2, \tag{1}$$

$$F(\xi\eta\zeta) = \sum_{n_1}\sum_{n_2}\sum_{n_3} F_o(\xi\eta\zeta)\exp[2\pi i(\xi n_1+\eta n_2+\zeta n_3)] \times \exp[2\pi i(p_1\xi+p_2\eta+p_3\zeta)] \times \sin 2\pi(\phi_1 n_1+\phi_2 n_2+\phi_3 n_3), \tag{2}$$

where scattering vector $\mathbf{s}=2\pi(\xi\boldsymbol{a}^*+\eta\boldsymbol{b}^*+\zeta\boldsymbol{c}^*)$, $2\boldsymbol{k}_F=2\pi(\phi_1\boldsymbol{a}^*+\phi_2\boldsymbol{b}^*+\phi_3\boldsymbol{c}^*)$, and $F_o(\xi\ \eta\ \zeta)$ is the scattering amplitude of the averaged structure without modulation wave. $I(\xi\ \eta\ \zeta)$ can be written as follows by the use of Bessel functions which satisfy the equation $\exp[x/2-(t-t^{-1})]=\sum_{n=-\infty}^{\infty} J_n(x)t^n$. Intensities of main reflections and satellite reflections $I(\xi\ \eta\ \zeta)$ can be written

$$I(\xi\eta\zeta) \propto |F_o(hkl)|^2 J_o^2[2\pi(p_1h+p_2k+p_3l)]\cdots\cdots(hkl) \tag{3}$$

$$\propto |F(h+m\phi_1, k+m\phi_2, 1+m\phi_3)|^2 \times J_m^2\{2\pi[p_1(h+m\phi_1)+p_2(k+m\phi_2)+p_3(l+m\phi_3)]\}\cdots\cdots(h+m\phi_1, k+m\phi_2, l+m\phi_3). \tag{4}$$

The intensities of the m-th satellite spots are proportional to the square of the m-th Bessel functions. In the case of $2\pi(\phi_1\boldsymbol{a}^*+\phi_2\boldsymbol{b}^*+\phi_3\boldsymbol{c}^*)=2\boldsymbol{k}_F$ the first satellite reflections are called $2k_F$ spots and the second satellite reflections appear at the $(h+4\pi\phi_1,\ k+4\pi\phi_2,\ l+4\pi\phi_3)$ in the reciprocal space. Since the amplitude of the periodical lattice modulation wave is small, $2\pi(p_1\xi+p_2\eta+p_3\zeta)(=x)$ is much less than 1.0 and $J_o(x)^2 \gg J_1(x)^2 \gg J_2(x)^2 \gg \cdots$. Therefore the intensities of the higher order satellite reflections are much smaller than those of the 1-st order satellite reflections. In facts, 2-nd order reflections can be scarecely seen on the Weissenberg photographs. When $x \ll 1$, $J_1(x)\simeq(1/2)x$ and the intensity formula becomes very simple.

If the periodical lattice distortion wave of α-LiPt(mnt) can be described in terms of the simple sinusoidal wave, A, defined by the following equation,

$$A = \sum_{\xi\eta\zeta}(|F_{obs}(\xi\eta\zeta)| - kS(\xi\eta\zeta)|F_{calc}(\xi\eta\zeta)|\times 2\pi(p_1\xi+p_2\eta+p_3\zeta)/2)^2$$

must be minimized. $F_{obsd}(\xi\ \eta\ \zeta)$ is an observed structure amplitude of the first order satellite reflection. $F_{calcd}(\xi\ \eta\ \zeta)$ is a structure amplitude calculated from the atomic parameters of the average structure and $S(\xi\ \eta\ \zeta)(=\mathrm{sign}(p_1\xi+p_2\eta+p_3\zeta))$ was easily determined by the examination of the intensity distribution of the 1337 satellite reflections. The conditions for the data collection were the same as those used in

determining the average structure at 153 K.

Figure 5 shows the examples of the intensity distributions of the observed structure amplitude of $|F(h+\phi_1, k+\phi_2, l+\phi_3)|$. The distribution of the $|F(\xi\ \eta\ \zeta)|$ is divided into two regions where the values of the $|F(\xi\ \eta\ \zeta)|$ are not zero. The position of this boundary changes according to ζ and forms a plane in the three dimensional reciprocal space. The intensities of satellite reflections are proportional to $|J_1(x)|^2$. When x is constant, $2\pi(p_1\xi+p_2\eta+p_3\zeta)(=x)$ represents one plane and intensities of satellite reflections are zero at the points of the reciprocal space where $(p_1\xi+p_2\eta+p_3\zeta)=0$. The intensities become stronger according to the departure from this plane. The sign of the satellite reflection is changed on this plane. Thus $S(\xi\ \eta\ \zeta)$ values in one region are determined $+1$ and those in the other region are -1. On the whole the intensity of satellite reflection becomes weaker, when $(\xi\ \eta\ \zeta)$ departs from the origin of the reciprocal space. p_1, p_2, and p_3 are determined by the minimization of A. From $\partial A/\partial p_1=0$, $\partial A/\partial p_2=0$, $\partial A/\partial p_3=0$, we obtain

$$\sum_{\xi\eta\zeta}(|F_o|-\pi kS|F_c|(p_1\xi+p_2\eta+p_3\zeta))\xi = 0,$$
$$\sum_{\xi\eta\zeta}(|F_o|-\pi kS|F_c|(p_1\xi+p_2\eta+p_3\zeta))\eta = 0,$$
$$\sum_{\xi\eta\zeta}(|F_o|-\pi kS|F_c|(p_1\xi+p_2\eta+p_3\zeta))\zeta = 0. \quad (5)$$

We used the scale factor k obtained in the structure determination of the averaged structure at 153 K. Based on the 1337 satellite reflections, p_1, p_2, and p_3 were determined as 0.045 Å, 0.137 Å, and 0.060 Å. The phase parameters (ϕ_1, ϕ_2, ϕ_3) were determined from the positions where the satellite reflections have maximum intensities in the reciprocal space. The four-circle diffractometer was scanned varying the indices of the reflections at intervals of 0.01 around the main reflections in order to gain the diffraction maxima of the satellite reflections. The diffraction maxima corresponding to Eqs. 3 and 4 represent main and satellite reflections which appear regularly at intervals of $|\phi_1 a^*+\phi_2 b^*+\phi_3 c^*|$. The measurement of the coordinates of the reflections in the reciprocal space gave $\phi_1=0.0$, $\phi_2=0.15$, $\phi_3=0.59$. The reliability factor R of 1337 satellite reflections was 0.18. Considering that R was calculated on the basis of the considerably weak satellite reflections, this result is satisfactory. The modulation wave of α-LiPt(mnt) is shown in Fig. 6. The amplitude of the modulation wave of α-LiPt(mnt) is 0.14 Å, which is similar to those of $Rb_{1.67}[Pt(C_2O_4)_2]\cdot 1.5H_2O$ (Rb-OP)[11] and $K_{1.81}[Pt(C_2O_4)_2]\cdot 2H_2O$ (γ-K-OP).[12] Comparison of the struc-

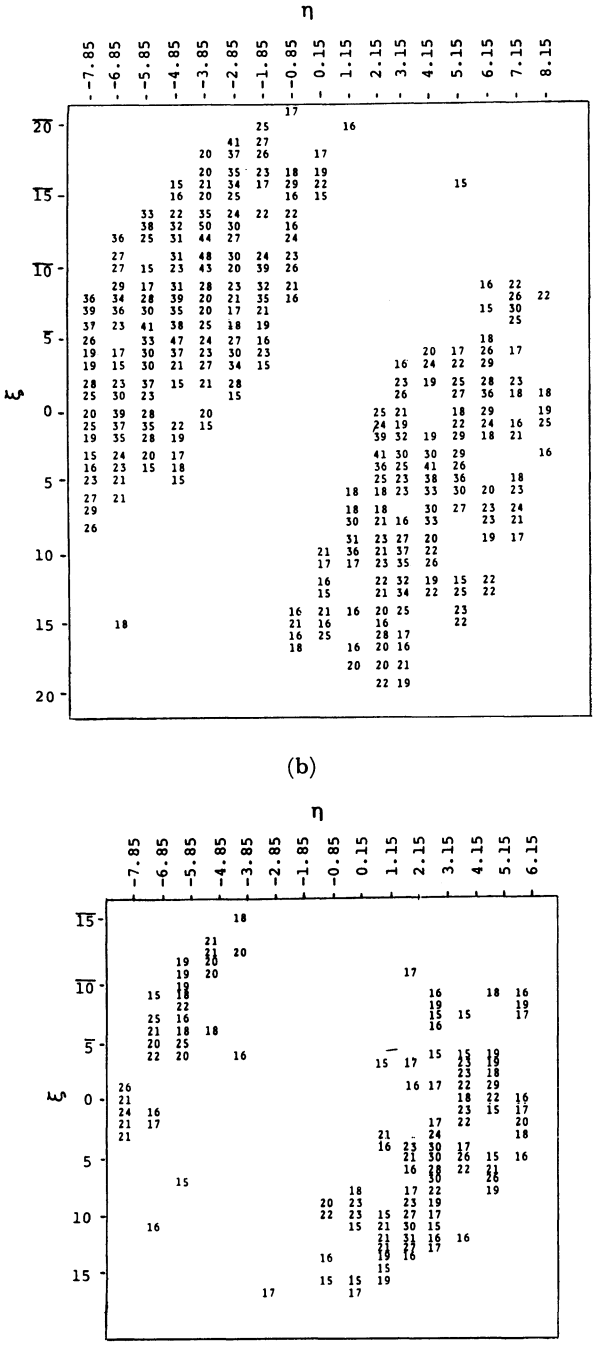

Fig. 5. Examples of the intensity distributions of the observed structure amplitudes of the satellite reflections, $|F(h+\phi_1, k+\phi_2, l+\phi_3)|$. The distribution of the $|F(\xi\eta\zeta)|$ is divided into two regions where the values of the $|F(\xi\eta\zeta)|$ are not zero. a): $\zeta=0.59$, b): $\zeta=2.59$.

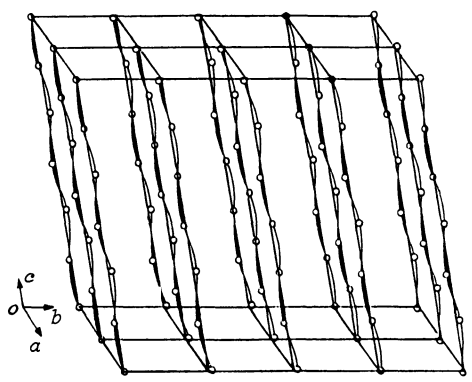

Fig. 6. Schematic drawing of the modulation wave of α-LiPt(mnt).

Table 6. Comparison of the superstructures of Pt complexes

	α-LiPt(mnt)	Rb-OP[11]	γ-K-OP[12]	KCP(Br)[13]
Chemical formula	$(H_3O)_{0.33}Li_{0.8}[Pt(mnt)_2]\cdot 1.67H_2O$	$Rb_{1.67}[Pt(C_2O_4)_2]\cdot 1.5H_2O$	$K_{1.31}[Pt(C_2O_4)_2]\cdot 2H_2O$	$K_2[Pt(CN)_4]Br_{0.3}\cdot 3H_2O$
Crystal System	Triclinic	Triclinic	Triclinic	Tetragonal
Pt···Pt Distance	3.597/Å	2.72, 2.83, 3.02/Å	2.84, 2.87/Å	2.89/Å
Modulation Wave	Transverse and Longitudinal	Longitudinal and Transverse	Transverse and Longitudinal	Longitudinal
Amplitude	0.14/Å(153 K) (0.045, 0.137, 0.060)/Å	0.17/Å(300 K)	0.17/Å(300 K) (0.20, −0.08, 0.11)/Å	0.02/Å(T<100 K)
Period	$2.38\times R_{Pt\cdots Pt}$(8.56/Å)	$6\times R_{Pt\cdots Pt}$(17.1/Å)	$10.5\times R_{Pt\cdots Pt}$(30.0/Å)	$6.5\times R_{Pt\cdots Pt}$(18.8/Å)
Order of the Chain Distortion	Complete Superstructure	Complete Sixfold Superstructure	Complete Supeestructure	Incomplete (Fluctuation of the Lattice Distortion)

Table 7. List of semiempirical parameters[14-16] (energy in eV)

		ζ	ε/eV			ε	ε/eV
C	2s	1.625	−21.4	N	2s	1.925	−26.0
	2p	1.625	−11.4		2p	1.925	−13.4
S	3s	2.122	−20.0	Pt	5d	*	−12.59
	3p	1.827	−11.0		6s	2.554	−9.077
	3d	1.5	−8.0		6p	2.554	−5.475

* double-ζ
$\chi = 0.6334\chi_1(6.013) + 0.5513\chi_2(2.696)$

Table 8. Intermolecular overlap integrals between the b_{3g} LUMO of the neutral molecules $[Pt(mnt)_2]^0$

S(**c**)*	-0.2365×10^{-1}
S(**b**)	-1.1189×10^{-2}
S(**b**+**c**)	0.3961×10^{-4}
S(**b**−**c**)	≈0

* S(m**b**+n**c**) indicates the overlap integral between the molecules located at (0, 0, 0) and (0, m**b**, n**c**).

tural data of the superstructures of platinum complexes is shown in Table 6. It may be of interest that in one-dimensional platinum complexes the lattice distortion wave gives rise to a periodical variation of the charge density along the Pt chains. The phase of the periodical distortion wave is considered to be governed by the interchain Coulomb coupling and the Pt chains are anti-phase ordered so as to minimize the Coulomb energy.[11] In α-LiPt (mnt), anti-phase ordering does not hold, perhaps due to the fairly strong transverse S···S interactions.

MO Calculation. We calculated the intermolecular overlap integrals(S) between LUMO of the neutral $Pt(mnt)_2$ molecule, obtained by means of the extended Hückel method. The molecule was idealized to have D_{2h} symmetry. The overlap integrals were calculated from Slater type orbitals. The semiempirical parameters are listed in Table 7. The overlap integrals along the face-to-face stacking direction are much larger than the interstack overlap integrals. The LUMO of the neutral $[Pt(mnt)_2]^0$ is b_{3g}, which agrees with the results of Schrauzer[17] and Yamatera.[18] Further the LUMO is consistent with the change of the bond distances obtained by the structure determination of $Ni(mnt)_2^{2-}$ and $Ni(mnt)_2^{1-}$.[10] The overlap integral of dz^2 orbital in the platinum chain in α-LiPt(mnt) is one-tenth of those of one-dimensional platinum complexes of tetracyanates or bisoxalates because of the large Pt··· Pt distance in α-LiPt(mnt). On the other hand, the intrastack overlap integrals of S atoms are the same order as those of the dz^2 orbitals of tetracyanoplatinates or bis(oxalato)platinates. The intermolecular overlap integrals between the b_{3g} LUMO of the neutral molecules were calculated and the values obtained are shown in Table 8. The overlap integrals along face-to-face stacking S(**c**) (intrastack) is much larger than the interstack overlap integrals S(***b***) or S(***b***+**c**), S(***b***−**c**). The large anisotropy indicates this compound is a one-dimensional metal. The value of S(**c**) indicates that the band width may be about 0.5 eV. Magnetic susceptibility measurements by J. R. Cooper show the conduction electron bandwidth ($4t_{//}$) in a tight binding model is 0.66 eV. This value is about a factor of 2.5 larger than that determined from the plasma frequency (0.26 eV).[6] The plasma frequency of this compound is much smaller than that observed for the usual platinum complexes of tetracyanates or bisoxalates.

Role of the Interchain Transverse S···S Contacts. The electrical conductivity of one-dimensional platinum complexes such as tetracyanoplatinates and bis(oxalato)platinates is strongly dependent on the periodicity of the Pt chain. Similar correlation between the electrical properties and the periodicity of the Pt chains can be also seen in $[Pt(mnt)_2]$ complexes. α-LiPt(mnt) is metallic at room temperature and at 213 K(T_c) a metal-insulator transition is observed. Since the $[Pt(mnt)_2]^{n-}$ are stacked regularly above T_c, the band is partially (59%) filled and one-dimensional metallic properties are observed. In $Rb[Pt(mnt)_2]\cdot 2H_2O$,[9] the band is half filled, which is consistent with the dimer structure and the semiconducting resistivity (≈10^5 Ωcm). In the case of β-LiPt(mnt)[8] the band is 1/4 (or 3/4) filled and the Peierls distortion produces a fourfold structure with a band gap at the Fermi level resulting in semiconducting properties which agree with the temperature dependence of its conductivity (≈10^{-3} Scm^{-1}). Though $M_x[Pt-$

$(mnt)_2$] has one-dimensional stacks of the platinum complexes, it cannot be regarded as typical one-dimensional system. In a one-dimensional system, the relationship between the band gap (2Δ) and the metal-insulator transition temperature (T_c) formed for the system without fluctuations, $2\Delta/T_c=3.73$, cannot be applied because the $2k_F$ lattice distortion does not develop until the temperature is lowered to as low as $T \lesssim T_c/3$ (hence $2\Delta/T_c \gtrsim 10$). In α-LiPt(mnt), $2\Delta/T_c$ is 3.95, which is close to the value derived from the mean field theory 3.73. The reason for the depression of the fluctuations of the lattice distortion wave lies in the characteristic interchain transverse contacts due to S atoms. Thus, despite of the one-dimensional nature of the electronic structure, α-LiPt(mnt) does not behave as one-dimensional system in the presence of the lattice distortion mode.

This work was supported by the Grant-in-Aid for special Research Projection "The Properties of Molecular Assembly" (No. 58218008), from the Ministry of Education, Science and Culture.

References

1) J. S. Miller and A. J. Epstein, *Prog. Inorg.Chem.*, **20**, 1 (1976).

2) J. S. Miller and A. J. Epstein, *J. Coord. Chem.*, **8**, 191 (1979).

3) J. W. Bray, H. R. Hart, J., L. V. Interrante, I. S. Jacobs, J. S. Kasper, P. A. Piacente, and G. D. Watkins, *Phys. Rev. B*, **16**, 1359 (1977).

4) A. E. Underhill and M. M. Ahmad, *J. Chem. Soc., Chem. Commun.*, **1981**, 67; M. M. Ahmad and A. E. Underhill, *J. Chem. Soc., Dalton Trans.*, **1982**, 1065; M. M. Ahmad, D. J. Turner, A. E. Underhill, C. S. Jacobsen, K. Mortensen, and K. Carneiro, *Phys. Rev. B*, **29**, 4796 (1984).

5) A. Kobayashi, Y. Sasaki, H. Kobayashi, A. E. Underhill, and M. M. Ahmad, *J. Chem. Soc., Chem. Commun.*, **1982**, 390.

6) J. R. Cooper, M. Miljak, M. M. Ahmad, and A. E. Underhill, *J. de Physique*, **44**, 1391 (1984).

7) A. E. Underhill and P. E. Clemenson, to be published. Recent investigation of average charge on the anion by treating the compound with an excess of iodine and back titrating the iodine with sodium thiosulphate, showed that the average charge on the anion appears to be 1.15. Further pH titrations on solutions of the salt revealed that there are approximately 0.33 protons per platinum in two different samples. Elemental analysis of Li was performed and the contents of Li was obtained as 0.75 with the aid of atomic emission spectrometry. On the other hand, we observed $2k_F$ satellite spots to appear on the layer lines of $(0.41\pm n)c^*$, or $(0.59\pm n)c^*$ (n=0,1,..) on the oscillation photograph around the c-axis. From the X-ray experiment total charge of the anion is supposed to be 0.82 or 1.18. The value of 1.18 is good agreement with the value of 1.15 obtained from the chemical analysis. Therefore the chemical formula of α-LiPt(mnt) is considered to be $(H_3O)_{0.33}Li_{0.8}[Pt(mnt)_2]\cdot 1.67H_2O$.

8) A. Kobayashi, Y. Sasaki, H. Kobayashi, A. E. Underhill, and M. M. Ahmad, *Chem. Lett.*, **1984**, 305.

9) M. M. Ahmad, D. J. Turner, A. E. Underhill, A. Kobayashi, Y. Sasaki, and H. Kobayashi, *J. Chem. Soc., Dalton, Trans.*, in press.

10) A. Kobayashi and Y. Sasaki, *Bull. Chem. Soc. Jpn.*, **50**, 2650 (1977).

11) A. Kobayashi, Y. Sasaki, and H. Kobayashi, *Bull. Chem. Soc. Jpn.*, **52**, 3682 (1979).

12) H. Kobayashi, I. Shirotani, A. Kobayashi, and Y. Sasaki, *Solid State Commun.*, **23**, 409 (1977); "Extended Linear Chain Compounds, Vol. 2," ed by J. S. Miller, Plenum Press, New York and London (1982).

On the basis of the intensity formula and the properties of Bessel funtions $J_m^2(X)=1$, some simple relations between Bessel functions and the relative intensities of the main and satellite reflections are derived. In the case of $K_{1.81}[Pt(C_2O_4)_2]\cdot 2H_2O$ we obtained the amplitude of the modulation wave using these simple relations. Satellite reflections were recorded on equi-inclination Weissenberg photographs and visually estimated.

13) J. W. Lynn, M. Iizumi, and G. Shirane, *Phys. Rev. B*, **12**, 1154 (1975).

14) R. S. Somnerville and R. Hoffman, *J. Am. Chem. Soc.*, **98**, 7240 (1976).

15) E. Clementi and D. J. Raimondi, *J. Chem. Phys.*, **38**, 2686 (1963).

16) H. Basch and H. B. Gray, *Theor. Chim. Acta*, **4**, 367 (1966).

17) G. N. Schrauzer and V. P. Mayweg, *J. Am. Chem. Soc.*, **87**, 3585 (1965).

18) M. Sano, H. Adachi, and H. Yamatera, *Bull. Chem. Soc. Jpn.*, **54**, 2636 (1981).